Optical Pumping Method to Reduce Light Shift in a Vapor Cell Atomic Frequency Standard

M. Zhu
Agilent Technologies, 5301 Stevens Creek Blvd., Santa Clara, CA 95051, USA

***Abstract*— A novel optical pumping method is developed to reduce the light shift (AC Stark shift) in a vapor cell atomic frequency standard. The method uses the multiple excited state energy levels to cancel the total light shift. The collision-broadened linewidth in the optical transition is used to reduce the resultant influence of the laser frequency detuning. Experimentally, the laser beam polarization is used to reduce the intensity variation induced clock frequency shift while the buffer gas pressure is adjusted to reduce the laser frequency fluctuation induced clock frequency shift.**

I. Introduction

The light shift (AC Stark shift) is one of the limiting factors for the performance of the optically pumped vapor cell atomic frequency standard [1]. Due to the interaction between the atom and the applied electromagnetic field, the energy levels for the clock transition are shifted. Fig. 1A shows a

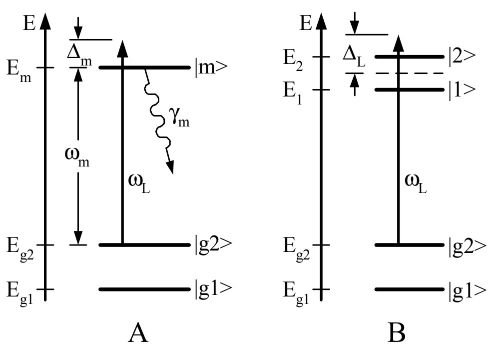

Figure 1. Energy diagram of a simplified atom

simplified atom interacting with a laser field. The laser angular frequency is ω_L. For the transition between the ground state |g2> and the excited state |m>, the Rabi frequency is Ω_m^{g2} and the detuning is $\Delta_m \equiv \omega_L - \omega_m$. The perturbation method [2] gives the energy shift of the state |g2> as

$$\delta E_{g2} \equiv \hbar\delta\omega_{g2} = \frac{\hbar}{4}\sum_m \frac{\left|\Omega_m^{g2}\right|^2 \Delta_m}{{\Delta_m}^2 + {\gamma_m}^2} \qquad (1)$$

where γ_m is the decay rate of the excited state |m>. When there is more than one optical frequency component in the laser field, e.g., in a coherent-population-trapping (CPT) configuration, the sum in (1) should include all the allowed transitions for all the optical frequency components. The observed clock frequency shift is

$$\delta\omega_{clock} = \delta\omega_{g2} - \delta\omega_{g1} \qquad (2)$$

which, in general, depends on both the laser intensity and the laser frequency.

Several methods have been developed to control the light shift in vapor cell based atomic frequency standards. In a population-altering-pumping (PAP) configuration, the optimum method used to eliminate the light shift is to pump the vapor cell using a pulsed light source [3] so that the atoms do not interact with the optical field when they are interrogated by the microwave field. In a CPT configuration, the total light shift averaged over the whole vapor cell can be suppressed by using the non-CPT-generating optical frequency components [4-6]. Another method is to modulate the optical intensity so that a servo system can control the total light shift by adjusting some operational parameters [7].

A new optical pumping configuration is presented here. This configuration reduces the dependence of the clock frequency on the laser intensity, the laser frequency, and the microwave power. In addition the laser frequency can be locked to the vapor cell directly.

II. Examples of Measured Light Shift

A. PAP configuration

Fig. 2 shows the measured light shift in a ^{87}Rb vapor cell. The D_2-line is used for optical pumping. The laser frequency is tuned to connect the |F = 2> ground state to the excited state $5p^2P_{3/2}$. In this case, the hyperfine structure in the excited state cannot be clearly resolved due to the Doppler broadening and collision broadening. The dispersion-like line shape shown in Fig. 2 is mainly determined by the energy shift in the ground state |F = 2, m_F = 0> because of the large frequency detuning for the transition between the state |F = 1, m_F = 0> and the excited state. Fig. 2 also includes the transmitted laser beam power vs. the laser frequency. Notice that the minimum of the transmitted optical power does not happen at zero laser frequency detuning, which is the laser frequency corresponding to the zero light shift. If the laser frequency is locked to this minimum transmitted optical power using a conventional frequency-dithering and phase-sensitive-detection method, both the laser intensity fluctuation and the laser frequency fluctuation will cause the fluctuation of the clock frequency between the states |F = 2, m_F = 0> and |F = 1, m_F = 0>. Also in this PAP configuration, the change of the microwave power changes the ground state population distribution, which in turn changes the laser beam intensity distribution in the optically thick cell and the clock frequency.

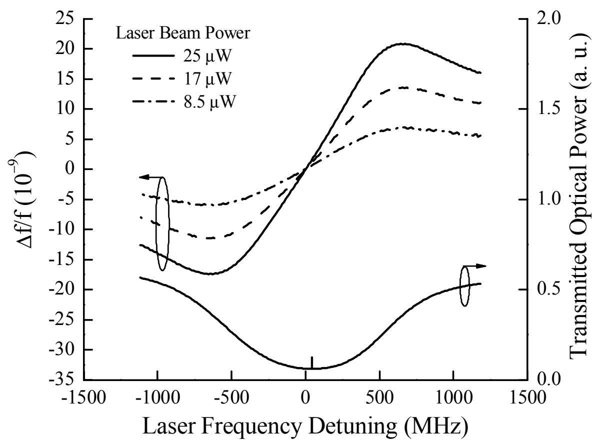

Figure 2. The measured light shift and transmitted optical power in a PAP configuration. The minimum of the transmitted optical power is marked by a short vertical line. See text for discussion.

B. *CPT configuration*

It has been demonstrated that the total light shift can be suppressed using the intensities and/or frequencies of the non-CPT-generating frequency components [4-6]. A convenient method is to use a frequency-modulated laser for CPT generation. The total light shift can be controlled using the modulation index. Fig. 3 shows the light shifts measured at

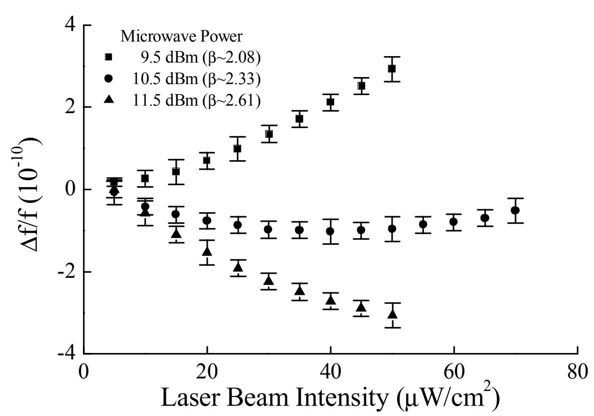

Figure 3. The measured light shift in a CPT configuration [4]. See text for discussion.

three different frequency modulation indices of the laser [4]. It is noticed that if one chooses the modulation index correctly, the light shift is compensated to zero averaged over the vapor cell. However, microwave power fluctuation causes the fluctuation in the clock frequency.

III. Light Shift in an Atom with Four Energy Levels

Fig. 1B shows an atom with four energy levels. The laser frequency ω_L is tuned to connect the ground state |g2> to the excited states |1> and |2>. According to (1), the energy shift of the state |g2> in the atom is given by

$$\delta E_{g2} \equiv \hbar\delta\omega_{g2} = \frac{\hbar}{4}\left\{\frac{\left|\Omega_1^{g2}\right|^2(\Delta_L+\omega_A)}{(\Delta_L+\omega_A)^2+\gamma^2}+\frac{\left|\Omega_2^{g2}\right|^2(\Delta_L-\omega_A)}{(\Delta_L-\omega_A)^2+\gamma^2}\right\} \tag{3}$$

where $\Delta_L \equiv \omega_L - \frac{1}{2\hbar}(E_1+E_2-2E_{g2})$ is the laser frequency detuning, and $\omega_A \equiv \frac{1}{2\hbar}(E_2-E_1)$ is one half of the frequency difference between the states |2> and |1>. In (3) the condition $\gamma_1 = \gamma_2 = \gamma$ is used. When the laser frequency detuning is kept at zero, i.e., $\Delta_L = 0$, (3) is simplified to the form

$$\delta E_{g2} \equiv \hbar\delta\omega_{g2} = \frac{\hbar\omega_A}{4}\frac{\left|\Omega_1^{g2}\right|^2-\left|\Omega_2^{g2}\right|^2}{{\omega_A}^2+\gamma^2} \tag{4}$$

Equation (4) shows that the light shift for the state |g2> is zero when the conditions $\Delta_L = 0$ and

$$\left|\Omega_1^{g2}\right| = \left|\Omega_2^{g2}\right| \tag{5}$$

are satisfied. Alternatively, both the sign and the amplitude of the light shift, δE_{g2}, can be readily changed by adjusting the Rabi frequencies of the two transitions. The absorption coefficient, α, due to the transitions from |g2> to |1> and |2> is a superposition of two Lorentzian line shapes, i.e.,

$$\alpha \propto \frac{1}{I_{laser}}\left\{\frac{\left|\Omega_1^{g2}\right|^2}{(\Delta_L+\omega_A)^2+\gamma^2}+\frac{\left|\Omega_2^{g2}\right|^2}{(\Delta_L-\omega_A)^2+\gamma^2}\right\} \tag{6}$$

where I_{laser} is the laser beam intensity. Equation (6) is symmetric with respect to $\Delta_L = 0$ when the condition (5) is satisfied.

The slope of the light shift shown in (3) is given by

$$\frac{\partial}{\partial\Delta_L}\delta E_{g2} = \frac{\hbar}{4}\left\{\left|\Omega_1^{g2}\right|^2\frac{\gamma^2-(\Delta_L+\omega_A)^2}{\left[\gamma^2+(\Delta_L+\omega_A)^2\right]^2} + \left|\Omega_2^{g2}\right|^2\frac{\gamma^2-(\Delta_L-\omega_A)^2}{\left[\gamma^2+(\Delta_L-\omega_A)^2\right]^2}\right\} \tag{7}$$

Equation (7) can be simplified at $\Delta_L = 0$. The result is

$$\frac{\partial}{\partial \Delta_L}\delta E_{g2}\Big|_{\Delta_L \to 0} = \frac{\hbar}{4}\left(\left|\Omega_1^{g2}\right|^2 + \left|\Omega_2^{g2}\right|^2\right)\frac{\gamma^2 - \omega_A{}^2}{\left(\gamma^2 + \omega_A{}^2\right)^2} \qquad (8)$$

It is seen from (8) that the slope of the light shift, δE_{g2}, at $\Delta_L = 0$ can be adjusted by changing the decay rate γ. When the condition $\gamma = \omega_A$ is satisfied, the slope of the light shift equals zero.

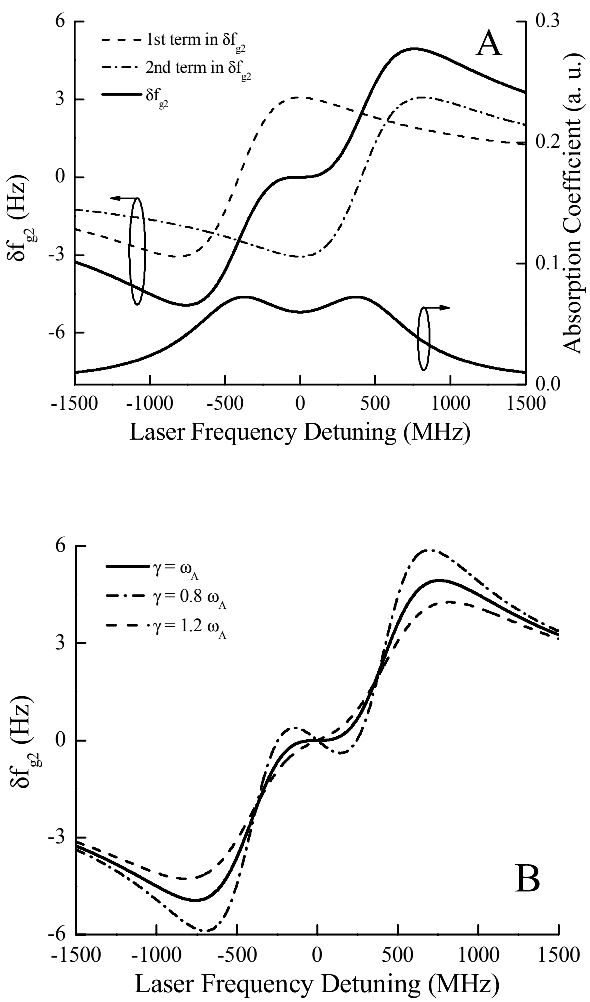

Figure 4. The calculated light shift and absorption using (3) and (6) for the four energy level atom shown in Fig. 1B. $\left|\Omega_1^{g2}\right| = \left|\Omega_2^{g2}\right| = 2\pi\times10^5$ rad./s and $\gamma = \omega_A = 2\pi \times 4.08 \times 10^8$ rad./s are used in the calculation. See the text.

Using the conditions $\left|\Omega_1^{g2}\right| = \left|\Omega_2^{g2}\right|$ and $\gamma = \omega_A$, Fig. 4A plots each contributing term in (3) as well as the resultant, $\delta f_{g2} \equiv \delta\omega_{g2}/2\pi$, vs. the laser frequency detuning Δ_L. It shows that the light shift $\delta\omega_{g2}$ is zero at $\Delta_L = 0$ when the condition (5) is satisfied. In addition, it shows that the slope of the light shift δf_{g2} is zero when $\gamma = \omega_A$ is satisfied. Fig. 4A also plots the total absorption coefficient (6) vs. the laser frequency detuning. The absorption coefficient shows a local minimum at $\Delta_L = 0$. Thus the laser frequency can be locked to this local minimum in the absorption coefficient of the cell directly. For comparison, Fig. 4B plots δf_{g2} for different values of γ. It shows that the slope of δf_{g2} at $\Delta_L = 0$ can be changed by changing the decay rate γ.

For the atom shown in Fig. 1B, the light shift for the ground state |g1>, δE_{g1}, is given by

$$\begin{aligned}\delta E_{g1} \equiv \hbar\delta\omega_{g1} &= \frac{\hbar}{4}\left\{\frac{\left|\Omega_1^{g1}\right|^2(\Delta_L - \omega_0 + \omega_A)}{(\Delta_L - \omega_0 + \omega_A)^2 + \gamma^2} + \frac{\left|\Omega_2^{g1}\right|^2(\Delta_L - \omega_0 - \omega_A)}{(\Delta_L - \omega_0 - \omega_A)^2 + \gamma^2}\right\} \\ &\approx \frac{\hbar}{4}\left\{\frac{\left|\Omega_1^{g1}\right|^2}{\Delta_L - \omega_0 + \omega_A} + \frac{\left|\Omega_2^{g1}\right|^2}{\Delta_L - \omega_0 - \omega_A}\right\} \\ &\approx -\frac{\hbar}{4}\frac{\left|\Omega_1^{g1}\right|^2 + \left|\Omega_2^{g1}\right|^2}{\omega_0}\end{aligned} \qquad (9)$$

where $\omega_0 \equiv \frac{1}{\hbar}\left(E_{g2} - E_{g1}\right)$ is the clock transition frequency. The first approximation in (9) uses the fact $\omega_0 >> \gamma$ while the second approximation is true for the case $\omega_0 >> \omega_A$ and $\Delta_L = 0$. Each term in (9) has a smaller absolute value and a smaller absolute slope than that of the corresponding term in (3) in the vicinity of $\Delta_L = 0$. Therefore the total light shift in the clock transition frequency, $\delta\omega_{g2} - \delta\omega_{g1}$, can be compensated to zero at $\Delta_L = 0$ by adjusting the ratio of the Rabi frequencies, $\left|\Omega_1^{g2}\right| / \left|\Omega_2^{g2}\right|$. Furthermore, the slope of $\delta\omega_{g2} - \delta\omega_{g1}$ at $\Delta_L = 0$ can also be compensated to zero by adjusting γ.

So far, the above discussion is limited to a single atom at rest. Obviously the results need to be integrated over all the velocity distributions. For an optically thick cell, which is the case for most vapor cell based atomic frequency standards, the resultant signal needs to be integrated along the cell length as well. However, the overall results are still true under these conditions, i.e., the total light shift and its slope in the vicinity of $\Delta_L = 0$ can be compensated to zero using the method discussed above.

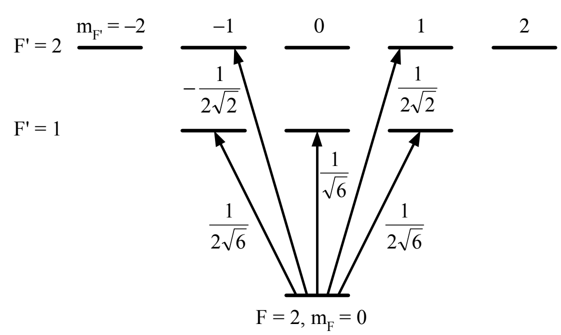

Figure 5. The electric dipole moment matrix elements related to the ground state |F =2, m_F = 0> in ^{87}Rb atom.

IV. EXPERIMENT RESULTS

The ^{87}Rb atom is chosen for the experiment. The ground states $|5s^2S_{1/2}, F = 2, m_F = 0\rangle$ and $|5s^2S_{1/2}, F = 1, m_F = 0\rangle$ are used for the clock transition. A single frequency laser with a wavelength of 795 nm is tuned to the resonance between the ground state $|5s^2S_{1/2}, F = 2\rangle$ and the excited states $|5p^2P_{1/2}, F' = 1, 2\rangle$. Thus the light shift of the ground state $|F = 2, m_F = 0\rangle$ plays a more important role than the one of the ground state $|F = 1, m_F = 0\rangle$ for the reasons discussed in Section III.

Fig. 5 shows the electric dipole moment matrix elements associated with the state $|5s^2S_{1/2}, F = 2, m_F = 0\rangle$ to the $5p^2P_{1/2}$ excited state. One convenient method to cancel the light shift using the method described in Section III is to choose the laser beam polarization. For example, when the linear polarization is chosen, with respect to the direction of the bias magnetic field, as

$$\hat{e} = \frac{1}{\sqrt{3}}\left(\hat{\pi} + \hat{\sigma}_+ + \hat{\sigma}_-\right) \tag{10}$$

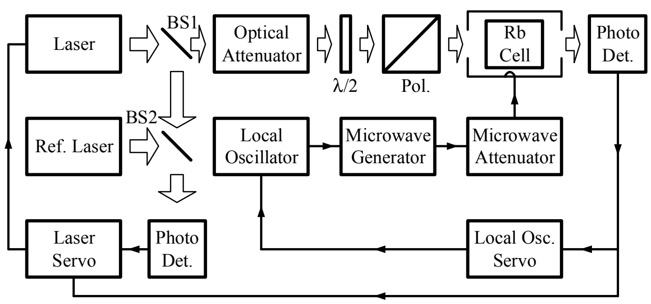

Figure 6. Experiment setup. Pol. is a linear polarizer. BS1 and BS2 are beam splitters. λ/2 is a half waveplate. The reference laser frequency is locked to a Rb cell using the FM saturation spectroscopy method.

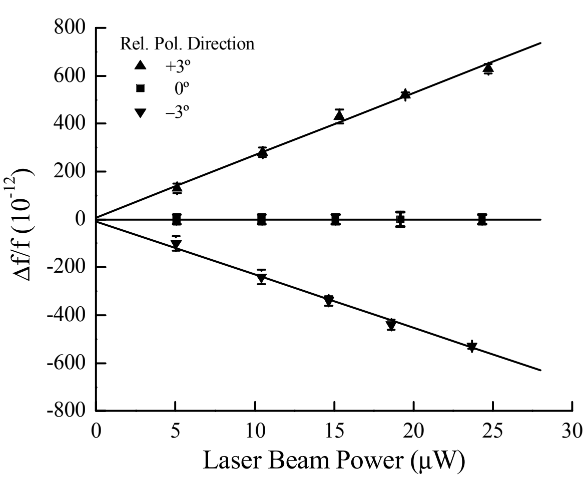

Figure 7. The measured clock frequency vs. laser beam power at different polarization angles. The solid lines are the results of the linear fit.

the light shift of the state $|5s^2S_{1/2}, F = 2, m_F = 0\rangle$ is canceled when the laser frequency is tuned to the middle of the $|F' = 1\rangle$ and $|F' = 2\rangle$ excited states. The polarization needs to be slightly different from (10) to compensate the total light shift in the clock transition frequency.

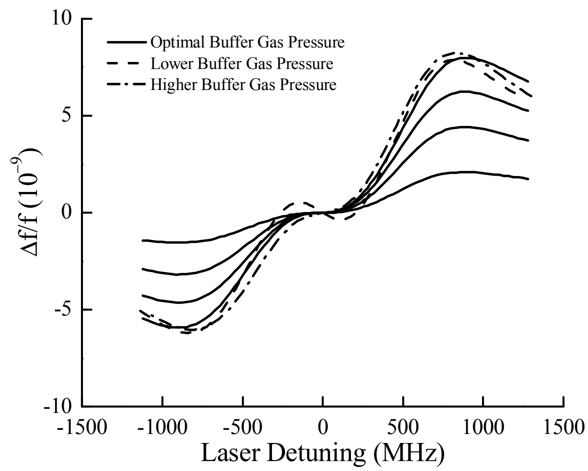

Figure 8. The measured light shift vs. laser frequency detuning in three cells. For the cell with the optimal buffer gas pressure, the laser beam powers are 5 μW, 10 μW, 15 μW and 20 μW. The laser beam powers are 20 μW for the other two cells.

It should be mentioned that the total absorption from the ground state $|F = 2\rangle$ is the sum of the contributions from all the Zeeman states. Therefore changing the polarization does not change the symmetric lineshape of the absorption.

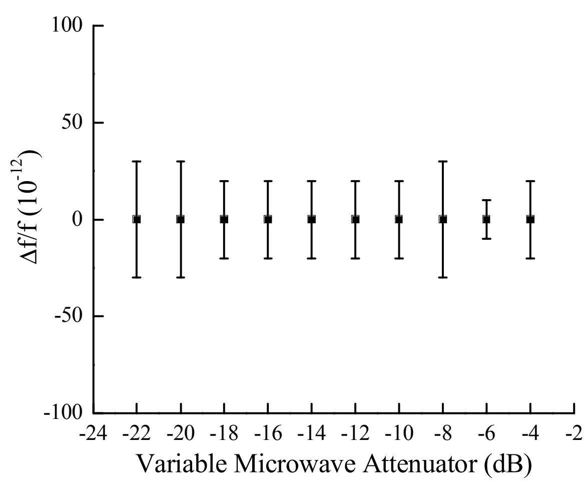

Figure 9. The measured clock frequency vs. the microwave variable attenuator settings. The laser frequency is locked to the local maximum of the transmitted laser beam power. The laser beam power is 10 μW.

The collision between the Rb atom and the buffer gas molecules increases the decay rate of the excited state $5p^2P_{1/2}$, and broadens the homogeneous linewidth of the transition between the ground state $5s^2S_{1/2}$ and the excited state $5p^2P_{1/2}$.

The linewidth (HWHM) of this transition, $\gamma/2\pi$, can be easily changed from ~3 MHz to >1 GHz by controlling the buffer gas pressure in the absorption cell. Thus the buffer gas pressure is used to compensate the slope of the light shift in the clock transition frequency.

Fig. 6 depicts the experimental setup. Several ^{87}Rb cells (ϕ ~ 14 mm, length ~18 mm) with different buffer gas pressures are used in the experiment. A diode laser with a wavelength of 795 nm is used for the optical pumping. The laser frequency is locked to the local peak of the transmitted laser power. Alternatively, the laser frequency can be locked to a reference laser with an offset frequency. A linear polarizer with a high extinction ratio is used to define the polarization of the laser beam before it enters the absorption cell. In addition a $\lambda/2$ waveplate in front of the polarizer adjusts the polarization of the laser beam. The microwave power fed into the oven/cavity combination is controlled by a microwave adjustable attenuator.

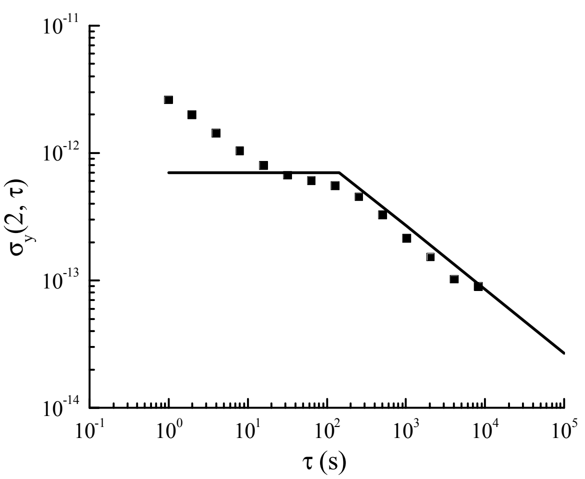

Figure 10. Allan Deviation of the experimental setup. ■ is the measured data. The solid line is the expected Allan Deviation of the reference system.

Fig. 7 shows the measured relative clock frequency vs. the laser beam power at three polarization angles. The laser frequency is locked to the local maximum of the transmitted laser beam power. It shows that the measured clock transition frequency is not sensitive to the change of the laser beam power when the polarization is set correctly.

Fig. 8 shows the relative clock frequency vs. the laser frequency detuning in three cells with different buffer gas pressures. It indicates that the slope of the light shift near zero laser frequency detuning can indeed be adjusted to zero when the buffer gas pressure is chosen correctly.

With the light shift under control, the clock frequency is measured vs. the microwave power (Fig. 9). As predicted by the lowest order of the theory [8], microwave power has no direct influence on the clock transition frequency.

Fig. 10 shows the Allan Deviation of this experimental setup. At ~100s the short term stability is limited by the reference system, while at $>10^4$s it is limited by the non-optimized buffer gas temperature coefficient for the cells used in the preliminary experiments.

V. SUMMARY

A novel optical pumping configuration is proposed and verified by the preliminary experiments. This method uses the hyperfine structure in the excited state of the atom to cancel the light shift, and it uses the collision broadened optical transition linewidth to reduce the light shift slope (vs. the laser frequency) in the vicinity where the laser frequency is locked for clock operation.

ACKNOWLEDGMENT

The author thanks Len Cutler for his managerial support of this project. The author is grateful to Jim Johnson, Ray Wong, and Jerry Amaral for their help with building parts for this project. The author thanks Jim Johnson and Curt Flory for reading this manuscript carefully and providing many suggestions.

REFERENCES

[1] See, for example, J. Vanier and C. Audoin, *The Quantum Physics of Atomic Frequency Standards*, Adam Hilger, (1989).

[2] See, for example, L. Schiff, *Quantum Mechanics*, McGraw-Hill, (1968).

[3] A. Godone, F. Levi, S. Micalizio, E. K. Bertacco, and C. E. Calosso, IEEE Trans. Instrum. Meas., **56**, 378, (2007).

[4] M. Zhu and L. S. Cutler, *Proceedings of the 32nd Annual Precise Time and Time Interval Systems and Applications Meeting*, p. 311, (2000).

[5] M. Zhu and L. S. Cutler, US Patent 6,201,821 (2001).

[6] M. Zhu and L. S. Cutler, US Patent 6,363,091 (2002).

[7] See, for example, V. Shah, V. Gerginov, P. D. D. Schwindt, S. Knappe, L. Hollberg, J. Kitching, Appl. Phys. Lett., **89**, 151124 (2006).

[8] M. Zhu, unpublished.